DOI: 10.4408/IJEGE.2011-03.B-087

GEOMORPHIC CHANGES OF A LANDSLIDE DAM BY OVERTOPPING EROSION

K. YOSHINO(*), T. UCHIDA(*), T. SHIMIZU(*) & K. TAMURA(*)

(*) Incorporated Administrative Agency, Public Works Research Institute, Japan

ABSTRACT

Clarifying geomorphic changes to landslide dams following overtopping is important for mitigation of future disasters. Past modelling experiments have not provided adequate information about geomorphic and grain size distribution changes at landslide dams. We used field survey data, aerial photographs, and LiDAR imagery to analyze the geomorphic changes of a landslide dam formed during the 2008 Iwate and Miyagi inland earthquake and the effect of subsequent overtopping erosion on the dam morphology and grain size distribution of the sediments. Our field survey data showed clear evidence of armour coating in the stream bed. We used LiDAR data sets recorded before overtopping, shortly after overtopping, and around 120 and 140 days after overtopping to clarify geomorphic changes. Our LiDAR data analysis revealed that around 30% of sediment eroded by overtopping was deposited within about 200 m of the lower end of the landslide dam, and that after overtopping, erosion and deposition gradually returned the riverbed gradient to close to that which existed before the landslide. Moreover, we showed that near the flat head of the landslide dam, the erosional channel was narrow and deep. Farther downstream from the flat head, the erosional channel was shallower and wider.

***Key words**: landslide dam, overtopping erosion, LiDAR data*

INTRODUCTION

Outburst flooding due to overtopping failure of landslide dams can cause catastrophic events (e.g., Costa *et alii*, 1988; Korup, 2004). Understanding the processes of overtopping erosion and sediment transport is needed for future mitigation of the downstream effects of these phenomena. Since the 1980s, various numerical models have been used to analyze the processes of overtopping erosion (e.g., Takahashi *et alii*, 1987; 1993). To date, erosional processes at landslide dams have been examined mainly by hydraulic modelling experiments (e.g., Takahashi *et alii*, 1983; Mizuyama *et alii*, 1989; Oda *et alii*, 2006, 2007), with the governing equations of these numerical simulations being theoretical analyses derived from hydraulic models.

Since 2004, detailed investigations of overtopping of large-scale landslide dams formed by the 2005 Typhoon No. 14, the 14 June 2008 Iwate and Miyagi inland earthquake, and the 2004 Chuetsu earthquake have been published (Kato *et alii*, 2005; Osanai *et alii*, 2007; Satofuka *et alii*, 2010; Uchida *et alii*, 2009). Moreover, numerical simulation models have been verified by observed data (e.g., Mori *et alii*, 2010; Satofuka *et alii*, 2010). However, in modelling the processes of overtopping erosion in these studies, the pre-failure shape of the landslide dams was inferred from the volume and distribution of collapsed sediment. Therefore, although discharge rates were reproduced well by these numeri-

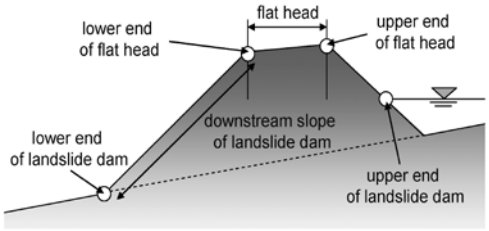

Fig. 1 - Schematic longitudinal profile of a landslide dam

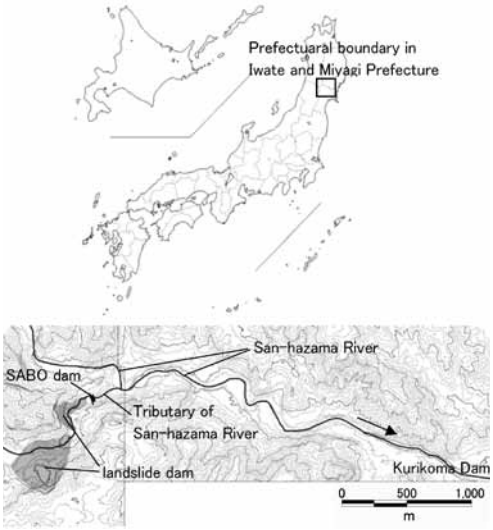

Fig. 2 - Regional location map and topographic map showing locations (grey shading) of two landslide dams in the Numakura-urasawa area. The larger of the two dams is the one investigated in this study. And contour interval are 10 m

cal simulations (e.g., Mori *et alii*, 2010; Satofuka *et alii*, 2010), the geomorphic change of landslide dam and the deposition of downstream of the dam were not adequately modelled.

Recent advances in LiDAR (Light Detection and Ranging) technology have allowed the acquisition of highly accurate topographic information that has been used to reveal the detailed geometry of landslide dams (e.g., Uchida *et alii*, 2009). In particular, detailed LiDAR-based measurements were taken shortly after formation of landslide dams triggered by the 2008 Iwate and Miyagi inland earthquake. Several of these landslide dams have since been breached by overtopping erosion and then re-measured using LiDAR data. These data allow us to see in detail the geomorphic change to landslide dams as a result of overtopping erosion.

Here we show new LiDAR data that demonstrate the geomorphic changes in response to overtopping erosion of a landslide dam on a tributary of the San-hazama River and the effects of downstream sediment erosion and deposition that followed. We investigated the detailed geometry of the water channel formed by overtopping and clarified the erosion processes involved. The terminology we use in this paper to describe the geometry of the landslide dam is as shown on the schematic longitudinal profile of Fig. 1.

STUDY SITE

We investigated a dam formed by a large landslide in the Numakura-Urasawa area during the 2008 Iwate and Miyagi inland earthquake (Fig. 2). The landslide

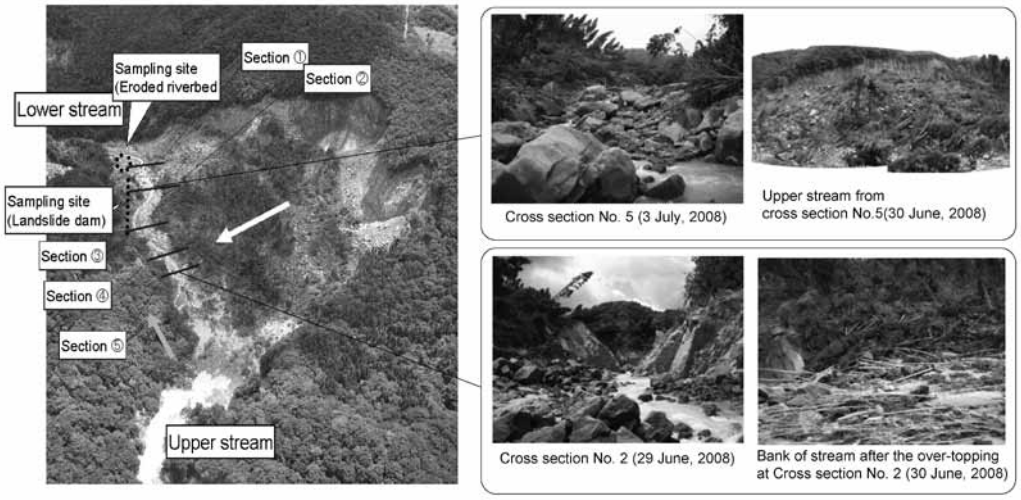

Fig. 3 - Landslide dam of Numakura-Urasawa after the overtopping

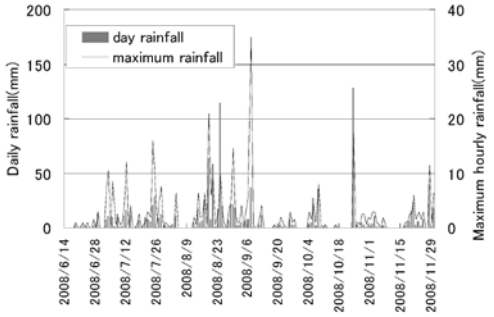

Fig. 4 - Hyetograph for the period 14 June- 29 November 2008 (AMeDAS data by Japan Meteorological Agency). Arrows indicate LiDAR data sets used in this study

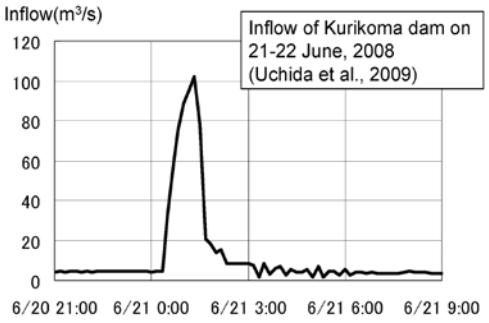

Fig. 5 - Water inflow rate for Kurikoma-Dam for 21-22 June 2008

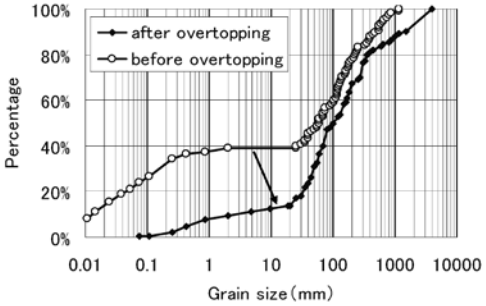

Fig. 6 - Grain size distribution of samples from the dam before overtopping and from the dam after overtopping Locations of sampling sites are shown in Fig. 3

dam formed on a tributary of the San-hazama River about 5 km upstream from Kurikoma Dam. There is also a small SABO dam (sediment control dam) about 450 m downstream of the lower end of the landslide dam. The landslide occurred on the valley slope above right side slope of the river channel. The catchment area upstream of the landslide dam is 18 km^2. The rainfall between 14 June (when the earthquake occurred) and the end of November is shown in Fig. 4. Maximum daily rainfall during this period was 128.5 mm (24 Oct.), and maximum hourly rainfall was 35 mm/h (7 Sep.).

There was no rainfall in the Numakura-Urasawa area from 20 to 21 June 2008, and overtopping erosion occurred on 21 June (Fig. 5.). At 0030 on 21 June 2008, discharge of water into the Kurikoma- Dam showed an exponential increase in response to overtopping of the landslide dam. At 0120 on 21 June, discharge into the dam peaked at about 100 m^3/s rate (Fig. 5.; Uchida *et alii*, 2009) We measured the grain size distributions of sediments from the landslide dam after overtopping and from the landslide dam before overtopping (Fig. 6). The ratio of sediment less than 2mm in the landslide dam after overtopping was smaller than that of the landslide dam before overtopping. Therefore, it shows armour coating due to overtopping erosion was clearly evident in the sample.

METHOD

DATA

We used three LiDAR data sets to provide information about the geometry of the landslide dam before the breach (data recorded 16 June), after the breach (8-9 September), and after heavy rainfall after the breach (12-13 November).

ANALYSIS

We defined the width of the river (riverbed and bank) from geomorphic features observed on LiDAR data, aerial photographs, and orthographic photo images (Fig. 7). We then determined the centre line of the river for measurements of longitudinal profiles of the riverbed. We also calculated a erosion and deposition amount for the river by taking the difference in altitude of two times LiDAR data set.

We measured the detailed geometry of the eroded water channel using the LiDAR data measured in September. First, we determined the extent of the eroded water channel from the difference between the riverbed cross sections of 16 June and 8-9 September (see Fig. 14). Then, we measured the widths at the bottom (B3) and top (B2) of the eroded channel, its depth (H), and the width of its banks (L) (see Fig. 7).

RESULTS AND DISCUSSION

GEOMORPHIC CHANGES TO AND NEAR THE LANDSLIDE DAM

Before the breaching, the longitudinal length of

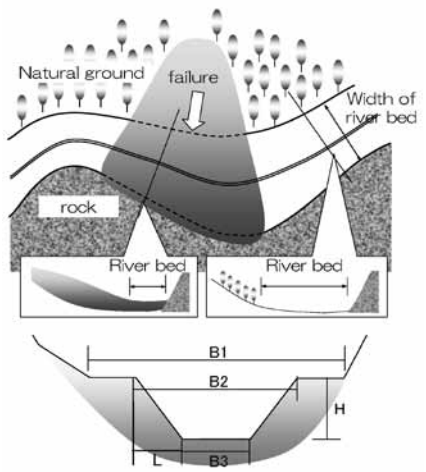

Fig. 7 - Schematic illustration of method used to define river width. The upper panel is a plan view; the two insets and the lower panel are cross sections

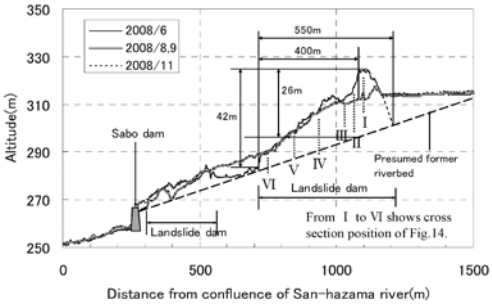

Fig. 8 - Geomorphic changes along a longitudinal section in the region of the landslide dam

the landslide dam was 550 m, the maximum height between the original riverbed level and the landslide dam surface was 26 m, and the height difference between the lower end of the landslide dam and its highest point was 42 m (Fig. 8). ponding occurred on the flat surface upstream of the landslide dam. Another, smaller landslide dam also formed 200 m downstream of the lower end of the large dam, but is not discussed in detail here. The longitudinal gradient of the large landslide dam surface between the lower end of the flat head and the lower end of the dam downstream slope of the landslide dam ranged from 2° to 10° and the mean gradient was 6° (Fig. 9).

Comparison of June and September LiDAR data showed that about 12 m of landslide debris was eroded at the flat head during overtopping (Fig. 10). The maximum erosion in the region 200 m immediately upstream from the lower end of the landslide dam was 2 m.

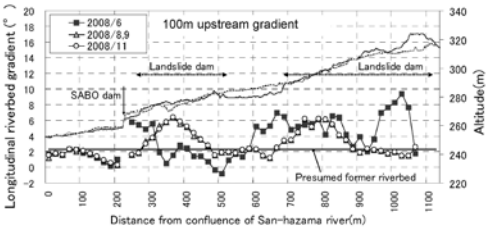

Fig. 9 - Longitudinal changes of riverbed gradient

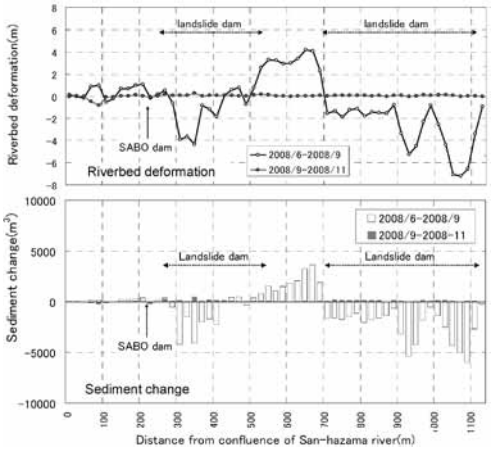

Fig. 10 - Longitudinal changes of riverbed deformation and of volumetric changes of deposition and erosion

The longitudinal gradient of the landslide dam surface between the lower end of the flat head and the point 200 m upstream from it was changed from 10° to 2° by overtopping erosion (Fig. 9). There was minimal change of the longitudinal gradient (6°) of the landslide dam surface between a point 200 m upstream from the lower end of the landslide dam and the lower end of landslide dam (Fig. 9).

Maximum deposition as a result of overtopping (4.2 m) occurred just downstream of the lower end of the landslide dam (upper panel of Fig. 10). The riverbed gradient in September in the area of deposition between the large and small landslide dams was almost the same as that of the initial riverbed (2.3°). There was less erosion or deposition (less than ~1 m) below the SABO dam than farther upstream. There were no remarkable changes in any part of the longitudinal profile during the September to November period (Fig. 8).

We calculated volumetric erosion and deposition at 20 m intervals along the profile for two periods (June-Sept and Sept- Nov; lower panel of Fig. 10). About 53,000 m^3 of sediments was eroded from the landslide

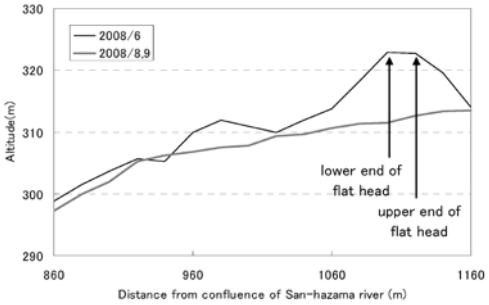

Fig. 11 - Longitudinal elevation profile of the centre line of the water channel

dam during June to September, and onethird of this sediment (18,000 m^3) was deposited between the lower end of the large landslide dam and the upper end of the small landslide dam. About 15,000 m^3 of sediment was eroded from the small landslide dam and about 2,000 m^3 of sediment was deposited between the small landslide dam and the confluence with the Sanhazama River.

GEOMORPHIC CHANGES OF THE WATER CHANNEL

The channel bed along the centre line of the water channel was eroded by about 12 m at the lower end of the flat head as a result of overtopping erosion (Fig. 11 and upper panel of Fig. 12). The depth of erosion generally decreased in the downstream direction (upper panel of Fig. 12). Longitudinal gradients of the channel bed along the centre line of the water channel were consistently around 2° from the upper end of the flat head to about 220 m downstream from there (Figg. 11 and 13).

We calculated the amount of erosion and deposition following overtopping by using the difference of the June and September LiDAR data, which we measured at 20 m intervals along the profile (lower panel of Fig. 12). From the upper end of the landslide dam to a point 150 m downstream (1,010 to 1,160 m in Fig. 12), the vertical amount of erosion corresponded with the volumetric change of sediment, whereas from 150 to 300 m downstream from the upper end of the dam (860 to 1,010 m in Fig. 12), the depth of erosion was relatively smaller, indicating that side bank erosion contributed to total erosion in this section of the profile (see also the 960 m cross section in Fig. 14). Vertical erosion occurred mainly at the flat head and on the upper part of the downstream slope of the landslide dam (1,010 to 1,160 m), whereas lateral erosion became dominant farther downstream.

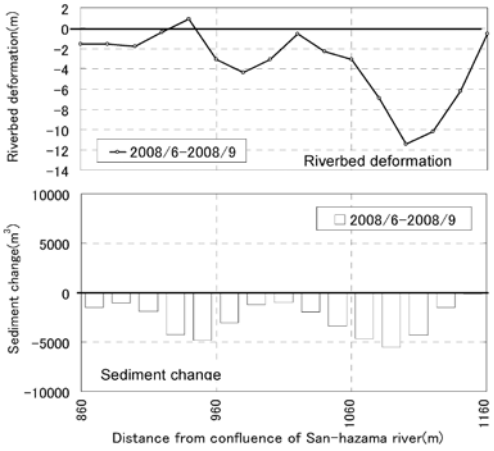

Fig. 12 - Longitudinal changes along riverbed centre line of riverbed deformation and of volumetric changes of deposition and erosion. Positive values indicate deposition and negative values indicate erosion

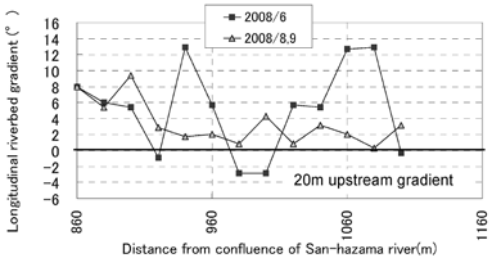

Fig. 13 - Longitudinal gradient profile along the centre line of the water

The widths of the bottom and the top of the eroded water channel (B3 and B2 of Fig. 7) were narrowest (about 15 and 40 m, respectively) around 40 to 100 m from the upper end of flat head (upper panel of Fig. 15) and increased gradually in the downstream direction. The greatest height of the eroded water channel (H of Fig. 7) was about 13 m near the flat head, and it decreased gradually in the downstream direction (middle panel of Fig. 15). The gradient of the side bank ranged from 10° to 45° (lower panel of Fig. 15). There was no clear trend in the relationship between the gradient of the side bank angle and distance along the profile.

The gradient of the side bank of the water channel varied considerably (by around 20°), despite the relatively constant height of the water channel (left panel of Fig. 16). The average gradient of the side bank was about 35°, regardless of the height of the water channel and the distance from the upper end of the flat head. The variations of the gradient of the side bank farther

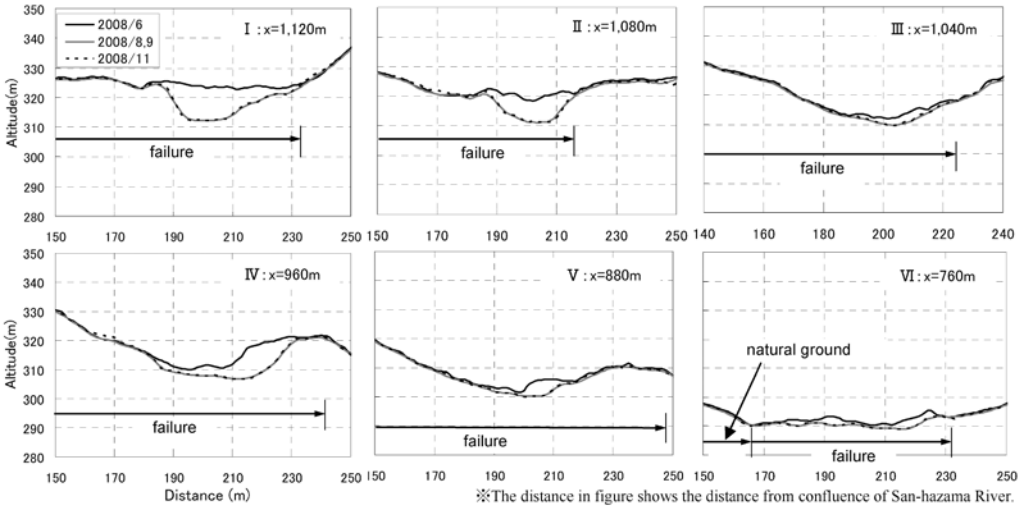

Fig. 14 - Changes of cross-section of eroded channel at six locations. Locations shown in Fig. 8

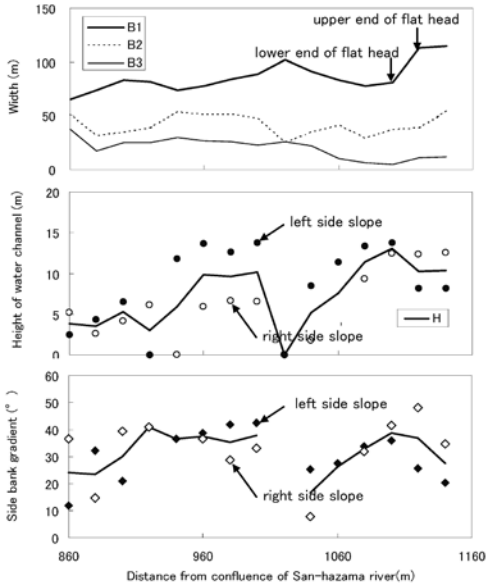

Fig. 15 - Longitudinal changes of width and height of water channel and of bank gradient

than 100 m from the upper end of the flat head were smaller than those within 100 m of it. The width of the side bank (L in Fig. 6) increased with increasing height of the water channel (middle panel of Fig. 16). The relationship between width of the bottom of the water channel and its height separated into two distinct clusters reflecting distance from the upper end of the flat head.

It was shown that the geomorphic change of a landslide dam and sediment deposition of the downstream by overtopping erosion ware shown in Fig. 17, Fig. 18. The depth of the eroded channel around the lower end of flat head is larger than the downstream. Moreover, the width of the eroded channel around the lower end of flat head is smaller than the downstream. On the other hands, slope gradient is almost constant between upstream and downstream. And it also almost constant between initial reverbed gradient and gradient at the deposited area by overtopping erosion.

CONCLUDING REMARKS

Our study revealed the following:

1. Approximately 30% of the sediment eroded by landslide dam overtopping was deposited within about 200 m of the lower end of the dam. After a landslide dam breach, erosion and deposition restored the riverbed's longitudinal gradient to conditions similar to those before the landslide dam formed.
2. The eroded water channel was narrow near the flat head and widened in the downstream direction. The water channel was shallowest near the flat head and deepened in the downstream direction. Erosion at the flat head and on the upper part of the downstream slope of the landslide dam was mainly vertical, whereas erosion was predominantly lateral farther downstream.

We conducted a detailed investigation of changes in sediment transport at, and downstream from, a landslide dam before and after dam overtopping. This investigation involved three sets of LiDAR data. We

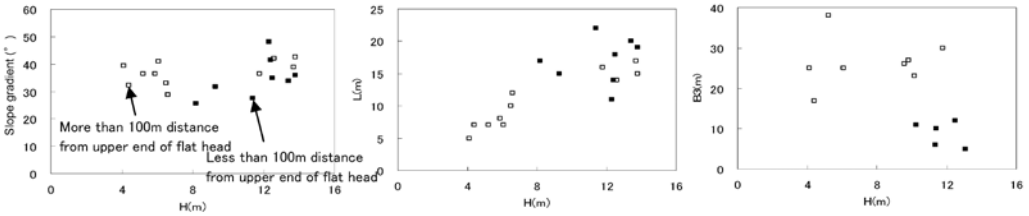

Fig. 16 - Relationships of height of the eroded water channel to the gradient of side bank (left panel), horizontal width (L) of the side bank (centre panel), and bottom width of the eroded channel (B3). Solid squares are from cross section less than 100 m from the upper end of the flat head, and open squares are from cross sections more than 100 m from the upper end of the flat head

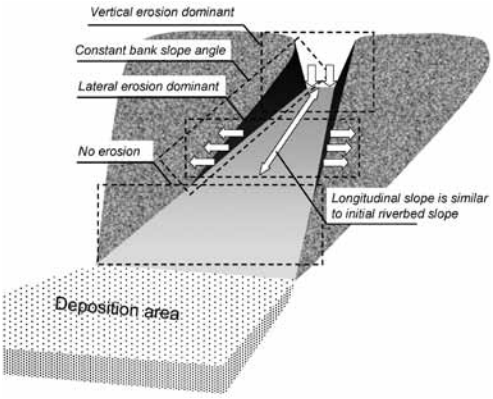

Fig. 17 - Schematic illustration of geomorphic change of the landslide and sediment deposition of the downstream

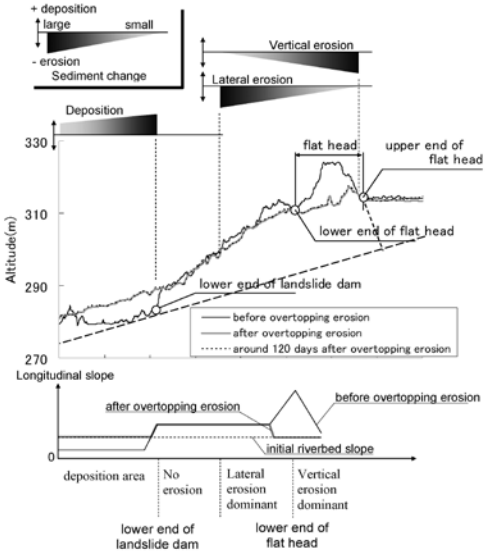

Fig. 18 - Schematic illustration of sediment change of the landslide and change of longitudinal riverbed slope

also examined how the geometry of the eroded water channel changed as a result of landslide dam overtopping, and analysed the erosion processes involved.

Future research will be required to verify our results, and should include hydraulic experiments and further investigations of the following issues:

- Depositional processes immediately downstream of landslide dams to assess the effects of various dam shapes and sizes.
- Armour coating and the influence of the water channel after a peak discharge is generated by erosion caused by landslide dam overtopping.
- How the physical properties of materials forming landslide dams (grain size, soil density, etc.) affect erosional processes.

ACKNOWLEDGEMENTS

The LiDAR data after the earthquake was offered by Miyagi Prefecture.

REFERENCES

Costa J.E. & Schuster R.L. (1988) - *The formation and failure of natural dams*. Geological Society of America Bulletin, **100**: 1054-1068.

Kato Y., Miyano T. & Mizuyama T. (2005) - *Outburst of small landslide dam on the Imokawa River* [prompt report], JSECE, **57**(6): 47-50. (in Japanese)

Korup O. (2004) - *Geomorphometric characteristics of New Zealand landslide dams*, Engineering Geology, **73**: 13-35.

Mizuyama T, Ishikawa Y. & Fukumoto A (1989) - *A Study on Failure of and Countermeasures against Landslide Dams*, Technical Memorandum of P.W.R.I., **2744**. (in Japanese)

Mori T., Sakaguchi T., Sawa Y., Mizuyama T., Satofuka Y., Ogawa K., Usuki N. & Yoshino K. (2010) - *Method of estimation for flood discharges caused by overflow erosion of landslide dams and its application in as a countermeasure*. Proceedings of the INTERPRAEVENT International Symposium in Pacific Rim, Taipei, Taiwan, 293-302.

Oda A., Mizuyama T., Hasegawa Y., Mori T. & Kawada T. (2006) - *Experimental study of process and outflow rate when landslide dams outburst.* JSECE, **59**(1): 29-34. (in Japanese)

Oda A., Mizuyama T. & Hasegawa Y. (2007) - *An experiment on a landslide dam outburst.* JSECE, **60**(2): 33-38. (in Japanese)

Osanai N., Uchida T. & Ito H. (2007) - *Real time Extraction Method for Natural dam Formation Triggered by Earthquake, Using the Lazar Profiler Surveying*. Civil Engineering Journal, **49**(9): 42-47. (in Japanese)

Satofuka Y., Mizuyama T., Ogawa K. & Yoshino K. (2010) - *Prediction of Floods Caused by Landslide Dam Collapse.* Journal of Disaster Research, 288-295.

Takahashi T. & Yagi H. (1983) - *Prediction of debris flow discharge*. Kyoto University Research Information Repository, **26**(B2): 329-351. (in Japanese)

Takahashi T., Nakagawa H. & Kuang, S. (1987) - *Estimation of debris flow hydrograph on varied slope bed.* Erosion and Sedimentation in the Pacific Rim, IAHS Publ., **165**: 167-177

Takahashi T. & Nakagawa H. (1993) - *Flood and Debris Flow Hydrograph Due to Collapse of a Natural Dam by Overtopping*, JSCE, **37**: 699-704. (in Japanese)

Uchida T., Matsuoka A., Matsumoto N., Matsuda J., Akiyama K., Tamura K. & Ichinohe K. (2009) - *Overtopping erosion of landslide dam at Numakura Urasawa, San-hazama river Miyagi Prefecture*. JSECE, **62**(3): 23-29. (in Japanese)